FORMATION OF THE SATURNIAN SYSTEM: A MODERN LAPLACIAN THEORY

A. J. R. PRENTICE

Department of Mathematics, Monash University, Clayton, Victoria, Australia

(Received 6 March, 1984)

Abstract. A theory for the formation of Saturn and its family of satellites, which is based on ideas of supersonic turbulent convection applied to the original Laplacian hypothesis, is presented. It is shown that if the primitive rotating cloud which gravitationally contracted to form Saturn possessed the same level of turbulent kinetic energy as the clouds which formed Jupiter and the Sun, given by $\frac{1}{2}\langle\rho_t v_t^2\rangle = \frac{1}{2}\beta\rho GM(r)/r$ where $\beta = 0.1065 \pm 0.0015$, then it would shed a concentric system of orbiting gas rings each of about the same mass: namely, $1.0 \times 10^{-3} M_S$. The orbital radii R_n ($n = 0, 1, 2, \ldots$) of these gas rings form a geometric sequence similar to the observed distances of the regular satellites. It is proposed that the satellites condensed from the gas rings one at a time, commencing with Iapetus which originally occupied a circular orbit at radius $11.4 R_S$. As the temperatures of the gas rings T_n increase with decreasing orbital size according as $T_n \propto 1/R_n$, a uniform gradient should be evident amongst the satellite compositions: Mimas is expected to be the rockiest and Iapetus the least rocky satellite. The densities predicted by the model coincide with the Voyager-determined values. Iapetus contains some 8% by weight solid CH_4. Titan is believed to be a captured satellite. It was probably responsible for driving Iapetus to its present distant orbit. Accretional time-scales and the post-accretional evolution of the satellites are briefly discussed.

1. Introduction

During the past 10 yr an attempt has been made to reformulate the original nebula hypothesis of Laplace (1796) relating to the formation of the solar system (Prentice, 1973, 1974, 1976, 1978a, b, 1980a, b, c, 1981a, b, 1983; Prentice and ter Haar, 1979a, b; Hourigan, 1977, 1981a, b). According to this theory, each of the planets of the solar system accreted from a concentric system of orbiting gas rings which had been shed by the primitive cloud which contracted to form the Sun. The idea was conceptually simple and readily able to account for the near circularity and coplanarity of the planetary orbits.

The Laplacian hypothesis was abandoned some 100 yr after its inception as a result of difficulties incurred in accounting for the observed distributions of mass and angular momentum in the solar system (Fouché, 1884). The problem is that most of the mass of the solar system lies with the Sun, and the Sun is spinning far too slowly for what Laplace proposed to have taken place. Of course, the Sun may have spun more quickly in the past. Even so, the mass of the planetary system is far too small compared with the mass of the material that would need to have been shed by the Sun for it to have safely contracted from the orbit of Neptune to its present size. Jeans (1928) pointed out that these circumstances could be reconciled only if the cloud which formed the sun rotated nearly uniformly, like a rigid body, and if most of its mass were concentrated near the centre.

Earth, Moon, and Planets **30** (1984) 209–228. 0167–9295/84/0303–0209$03.00.

In 1973, I put forward a set of calculations which indicated that if there has existed a large supersonic turbulent stress within the cloud of the form

$$\langle \rho_t v_t^2 \rangle = \beta \rho G M(r)/r, \tag{1}$$

where β is a dimensionless number of order 0.1, then the cloud would acquire the characteristics sought by Laplace, where ρ is the local gas density, $M(r)$ is the mass interior to radius r and β is called the turbulence parameter. It was proposed that the turbulent stress was created by the motions of large-scale convective elements which were accelerated to supersonic velocities by powerful buoyancy forces within the cloud. The positive buoyancy is due to the existence of a very steep superadiabatic temperature gradient. In that case, $\beta/2 \sim 0.05$ represents the fraction of the cloud's local gravitational energy which is stored as kinetic energy in turbulent convective motions.

Although the conventional mixing theory of convection does not admit the possibility of supersonic convective motions (Cox and Giuli, 1968; p. 293), studies of T Tauri-stars which are thought to be very young stars of solar mass do indicate the existence of very violent outbursts and winds from these objects, having speeds of order 100 km s^{-1} (Herbig, 1962). This is nearly 10 times the speed of sound in the gas and implies turbulent stresses having magnitude of order 100 times the normal gas pressure. At a workshop on T Tauri stars, Cohen (1981) concluded that now that the existence of a high flux of mechanical energy in the atmospheres of these objects has been firmly established, it is time that this phenomenon attracted some attention from theorists.

It is the purpose of this paper to present a modern Laplacian theory for the formation of Saturn and its family of regular satellites. A basic tenet of this theory is that the same physical mechanism was responsible for the formation of both the planetary and regular satellite systems. In particular, it is proposed that each of the clouds which formed Jupiter, Saturn, and the Sun possessed a common fraction of supersonic turbulent energy, reflected by the same value of $\beta \sim 0.1$.

The basic assumptions and equations of the theory are summarized in Section 2 below. In Section 2 we apply these equations to develop a detailed model of the proto-Saturnian cloud and its system of shed gaseous rings. The results of numerical computations based on this model, which yield the expected satellite compositions and densities, are presented in Section 4. In the final section of the paper we estimate the time scales governing the accretion of the satellites and discuss the relationship of the satellite mass distribution to the gas ring lifetimes. We also consider the thermal evolution of the satellites in the first few 10^8 yr of their existence and the origin of Titan, whose mass is far too great in the present scheme for it to be a naturally formed moon of Saturn.

2. The Modern Laplacian Theory

2.1. SHEDDING OF GAS RINGS

According to the modern Laplacian theory for the formation of the solar system (Prentice, 1978a, b; Prentice and ter Haar, 1979a, b; Prentice, 1981a, b), each of the

planets/regular satellites condensed from a concentric system of orbiting gaseous rings which were shed by the primitive gaseous envelopes which gravitationally contracted to form the central body. The orbital radii R_n of these rings of mass m_n, numbering inwards from the outermost one ($n = 0, 1, 2, \ldots$), are related to each other by the equations

$$\frac{R_n}{R_{n+1}} = \left(\frac{f_{n+1}}{f_n}\right)^2 \left(\frac{M_{n+1}}{M_n}\right)^3 \left[1 + \frac{m_{n+1}}{M_{n+1} f_{n+1}}\right]^2, \tag{2}$$

where M_n, f_n denote the mass and moment-of-inertia factor of the parent cloud after detachment of the nth gaseous ring. Equation (2) is simply the equation representing conservation of total angular momentum for the cloud-ring system.

The quantity f is defined such that $M_n R_n^2 f_n$ is the axial moment-of-inertia of the rotating cloud when the angular velocity at the equator equals the Keplerian value

$$\omega_n = \sqrt{GM_n/R_n^3}. \tag{3}$$

The value of f_n is sensitive to the amount of supersonic turbulent stress in the cloud. The turbulent stress increases outwardly with radius r, from zero at the centre to nearly 100 times the usual gas pressure $\rho \mathscr{R} T/\mu$ at the edge. Because of this non-uniform behaviour, the outer tenuous layers of the cloud are pushed outwards by the turbulent stress far more so than the inner dense regions, with the net result that the cloud appears very centrally condensed. Typically f falls by an order of magnitude from 0.1124 to 0.0106 as β increases from 0 to 0.1 in a non-rotating polytropic structure of index $n = 2.5$ (Prentice, 1973). Rotation reduces f by a further factor of 4/9. It should also be mentioned that the turbulence causes the cloud interior to rotate nearly uniformly through the generation of a large turbulent viscosity.

We now assume that the gravitational contraction of the cloud occurs uniformly and the turbulence is strong, so that both f and m_n/M_n remain constant and are small numbers. In that case, the residual cloud mass M_n remains nearly constant: i.e., $M_n \simeq M$, and the set of orbital radii r_n form a geometric sequence. We have

$$R_n/R_{n+1} = [1 + m/Mf]^2 \simeq \text{const.} \tag{4}$$

This is very similar to the Titius–Bode law of planetary distances (ter Haar, 1967).

2.2. PHYSICAL STRUCTURE OF THE GAS RINGS

The gas rings which are shed by the contracting cloud have a uniform specific angular momentum $h_n = \sqrt{GM_n R_n}$, implying a differential angular velocity distribution

$$\omega(s, z) = \omega_n (R_n/s)^2, \tag{5}$$

where (s, z) denote cylindrical co-ordinates referred to the axis of rotation of the parent cloud. If the gas is assumed to be isothermal, having temperature T_n and molecular weight μ, integration of its hydrostatic support equation yields the density distribution

$$\rho_n(\xi) = \rho_n \exp(-\tfrac{1}{2}\alpha_n \xi^2/R_n^2), \tag{6}$$

where ξ denotes meridional distance from the mean circular Keplerian orbit $s = R_n$. Here ρ_n denotes the gas density on the mean orbit and

$$\alpha_n = \mu G M_n / \mathscr{R} T_n R_n \simeq \mathscr{O}(10^2) \tag{7}$$

is a dimensionless number, essentially equal to the ratio of the gravitational potential energy to thermal energy of the gas.

If the gravitational contraction of the cloud takes place uniformly, then α_n is constant from one gas ring to the next, at the time of the ring detachment, apart from small changes induced by the steady dissociation of H_2 inside the cloud. For Saturn this dissociation effect is unimportant.

From Equation (6) it follows that the central density of the gas ring is related to its mass m_n according as

$$\rho_n = \alpha_n m_n / 4\pi^2 R_n^3. \tag{8}$$

Thus since the Titius–Bode equation (4) implies that m_n and M_n remain nearly constant when $f \ll 1$, it follows that T_n and ρ_n scale with orbital radius R_n according as

$$T_n \propto 1/R_n, \qquad \rho_n \propto 1/R_n^3. \tag{9}$$

The precise values of T_n and ρ_n depend on the choice of the parameters α_n, β and the mass of the cloud. Nonetheless, it is obvious from these equations that if the chemical composition of the regular satellites reflects the thermodynamic state of the gas rings, from which they are assumed to have condensed, then one would expect to see a well-defined compositional gradient, with the satellites becoming steadily rockier and denser moving towards the planet.

2.3. Gravitational Settling Out of the Condensate Material

A unique feature of the gas ring configuration is that all condensate grains automatically settle onto the mean circular Keplerian orbit R_n, irrespective of their point of origin in the gas ring, as schematically illustrated in Figure 1. This remarkable circumstance arises through a balance of the parent cloud's gravitational attraction with the centrifugal force induced through the orbital angular velocity distribution given by Equation (5). Gas drag causes the orbital angular velocity of the grain to match that of the gas at each stage of its descent onto the mean circular orbit R_n. Since all condensate material is focussed onto the one common orbit, there is no spatial fractionation of different chemical species. That is, each satellite is expected to be internally chemically uniform at the time of its accretion.

2.4. Formation of the Planetary Cores of the Major Planets

In the case of the planetary system, where the mean ratio of the orbital distances of the planets is $\langle R_n/R_{n+1} \rangle = 1.723$, it follows from Equation (4) that the mean mass of each gas ring is $1000\, M_\oplus$, taking $f = 0.01$. Such a mass of gas of solar composition (see Table I)

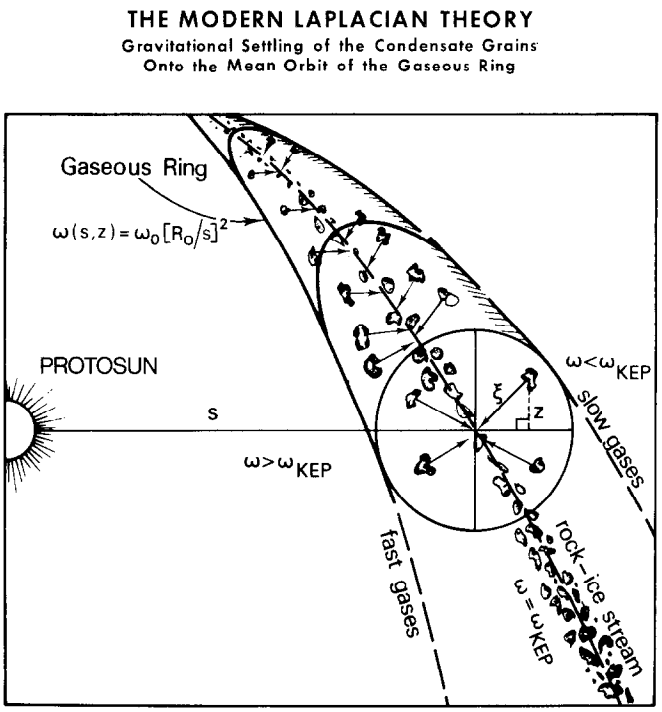

Fig. 1. Schematic view of a gaseous ring around the protosun, showing the gravitational settling of solid grains onto the mean circular orbit $s = R_0$, where the orbital angular velocity of the gas equals the local Keplerian value $\omega_0 \equiv \omega_{KEP} = (GM/R_0^3)^{1/2}$ (adapted from Prentice, 1974).

contains $5 - 19 M_\oplus$ of condensable rocks and ices, depending on the temperature of condensation.

The first stage in the formation of each planet is the settling out of the condensate grains onto the mean orbit of the gas ring, as described above, and the subsequent gravitational accumulation of this material along the mean orbit to form a dense planetary embryo, or core (Hourigan, 1977, 1981a, b; Prentice, 1974, 1980c). In the case of Saturn, the core consists of rock, H_2O ice and NH_3 ice and has a mass of order $14 M_\oplus$. The existence of planetary cores of roughly comparable mass at the centres of the major planets, as predicted by Equation (4), has been confirmed by a wide range of planetary model calculations (Slattery, 1977; Hubbard and MacFarlane, 1980; Grossman *et al.*, 1980) and spacecraft gravity data (Anderson *et al.*, 1980).

Whilst the rock-ice cores of the major planets are accumulating, a process which takes some $10^4 - 10^5$ yr (Prentice, 1978a), much of the mass of the gas ring is lost through thermal evaporation. This process is more pronounced with increasing orbital distance and results in a complete loss of gas from Neptune's orbit (Hoyle, 1960). Once the planetary cores have formed, however, they can act as a gravitational sink for the residual gases of the parent gas ring. It is through the capture of these rotating gaseous envelopes

TABLE I

Solar abundances and thermodynamic constants of the principal chemical species

Index i	Chemical species name	Abundance mass fraction $Z_{i,\odot}$	Density ρ_i (77 K) ($g\,cm^{-3}$)	A_i (K)	B_i
0	Anhydrous 'Io' rock	0.005 74	3.361	–	–
1	H_2O	0.009 50	0.934	2673.0	7.572
2	NH_3 (as $NH_3 \cdot H_2O$)	0.001 29	0.838	1765.6	6.258
3	CH_4 (as $CH_4 \cdot 5.75\ H_2O$)	0.001 47	0.507	911.1	4.440
4	CH_4 (total)	0.005 83	0.507	505.9	4.642

that the regular satellite systems of the major planets are formed, via the same physical processes of ring shedding and grain accumulation described above.

3. The Numerical Model

3.1. SPECIFICATION OF PARAMETERS

In order to compute the temperature and density of each gas ring it is necessary to specify the values of the parameters α_n and β. Prentice (1981a) has argued that as the second of these parameters is non-thermal in origin it is uninfluenced by the level of molecular dissociation in the gas. The same value of β may therefore have characterized the gravitational contraction of the 3 clouds which formed Jupiter, Saturn, and the Sun. Standardizing β against the observed chemistry of the planetary system yields a value $\beta = 0.1065 \pm 0.0015$, assuming the H and He mass fractions of the cloud to be $X = 0.8$ and $Y = 0.2$, respectively. These abundances are the ones indicated by the measurements of Gautier *et al.* (1981) at Jupiter. Of course, all of the primordial clouds are assumed to have the same X/Y ratio.

Prentice and ter Haar (1979a, b) found that values of β in the above range also account for the observed chemistry of the Galilean system of satellites, with X scaled to 0.8. For Saturn we therefore assume that

$$\beta = 0.1065. \tag{10}$$

The parameter α_n is fixed from the condition that the ratio R_n/R_{n+1} of orbital radii of successively detached rings matches the observed mean value: namely, 1.30, considering the satellites Mimas through Rhea. This yields

$$\alpha_n \simeq 225. \tag{11}$$

Once α_n and β are specified, the temperatures follow from Equation (7), noting the mean molecular weight of the gas to be $\mu = 2.222$. The masses M_n steadily decline as the gas rings of mass $m_n = M_{n-1} - M_n$ are discarded. The initial cloud mass M_0 is chosen so that the final mass equals $M_S = 5.686 \times 10^{29}$ g. Also, for the above choice of α_n and β we obtain $f_n = 0.007$, $m_n/M_n = 9.89 \times 10^{-4}$. Equation (8) can now be used to compute ρ_n.

The computed values of T_n, ρ_n and the pressure $p_n = \rho_n \mathscr{R} T_n/\mu$ on the mean orbit of the gas ring are listed in Table II.

3.2. INFLUENCE OF SOLAR RADIATION ON THE PROTO-SATURNIAN GAS RINGS

It should also be pointed out that the temperatures of the outermost gas rings are significantly influenced by heating due to the primordial Sun. T_n needs to be replaced by the value

$$T_n^* = [T_n^4 + (\mathscr{L}_i/\mathscr{L}_\odot) T_S^4]^{1/4}, \tag{12}$$

where $T_S \simeq 77$ K denotes the present solar temperature at Saturn's orbit (Lupo and Lewis, 1979) and $\mathscr{L}_i \simeq 0.4\,\mathscr{L}_\odot$ is the Sun's estimated luminosity on joining the Zero-Age Main Sequence (Prentice, 1976). This yields a background temperature $T_S' \simeq 60$ K at the time of Saturn's formation. It follows that the proto-Saturnian cloud cannot begin to establish itself thermodynamically, and shed discrete gas rings in the manner described above, unless $T_n > T_S'$ or, using Equation (7), until

$$R_n \leq 12.3\,R_S, \tag{13}$$

where $R_S = 6.033 \times 10^9$ cm denotes the present equatorial radius of Saturn. It is possible, therefore, that the cloud sheds one gas ring prior to reaching the orbital radius of Rhea, near radius $11.4\,R_S$.

3.3. ORBITAL RADII OF THE COMPLETE SYSTEM OF GAS RINGS

It is assumed that the gas rings were shed at the present satellite positions, with the exception of Iapetus and Titan. Iapetus, as we shall discuss below, is the satellite which formed from the first shed gas ring at orbital radius $R_0 = 11.4\,R_S$. Titan is believed to be a captured moon which drove out the newly formed Iapetus to its present orbital position, at radius $59\,R_S$ (see Section 5.3 below).

The process of shedding gas rings cannot proceed indefinitely since the temperature relation $T_n \propto 1/R_n$ leads to an unrealistically high value of 500 K for the present temperature of Saturn! We suggest that soon after the orbit of Mimas had been passed, at orbital radius $3\,R_S$, the surface temperature of the cloud began to fall progressively below the equivalent $1/R_n$ value. Concomitant with such a downturn in T_n is a steady decline in the degree of turbulence, measured by β, and the mass of material that can be shed in the form of gas rings.

Choosing a final surface temperature of 235 K, as shown in Figure 2, the cloud sheds gas rings at positions corresponding very closely to the mean orbits of the co-orbital satellites 1980 S1, 1980 S3 and of the shepherds 1980 S26, 1980 S27 as well as at the orbit of the innermost moonlet 1980 S28. The discrete process of ring shedding ceases altogether at the outer edge of the A ring ($2.27\,R_S$ – Stone and Miner, 1982). Below this radius any further material that is shed is done so continuously, forming a gaseous Keplerian disc in the equatorial plane of the receding globe. We suggest that Saturn's

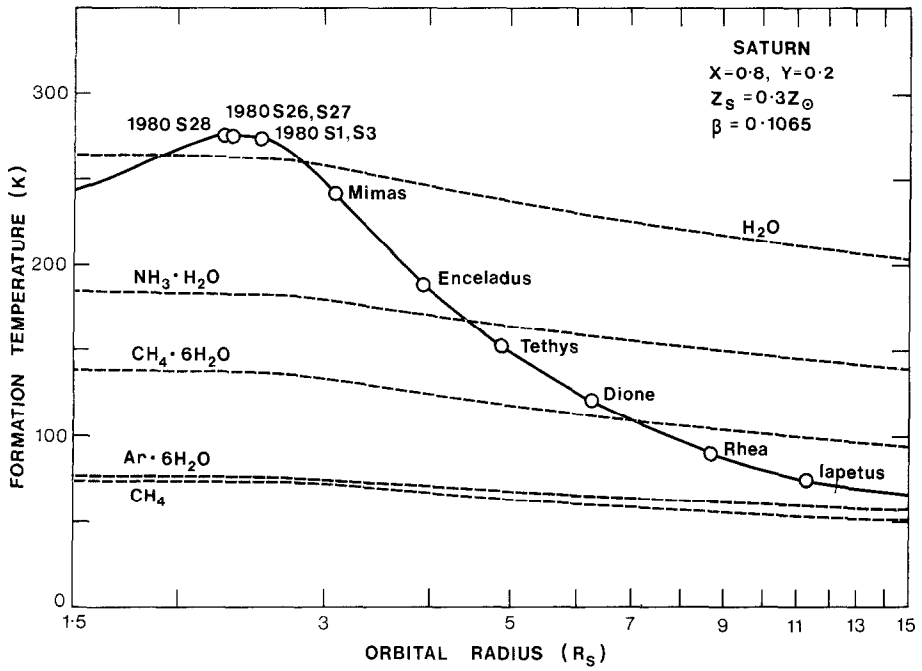

Fig. 2. Temperature at the equator of the contracting proto-Saturnian cloud, plotted as a function of cloud size expressed in units of $R_S = 6.033 \times 10^9$ cm. The small circles mark the positions of the regular satellites, with Iapetus having been assumed to form originally at orbital radius 11.4 R_S. The broken curves define the condensation temperature of the main chemical species, assuming the gas to have solar abundance proportions of heavy elements. They are computed for the gas pressure on the mean orbit of the gas ring just after detachment from the parent cloud.

icy rings formed through condensation within such a final remnant disc (cf. Pollack *et al.*, 1976).

4. Discussion of Numerical Results

4.1. Formation Temperatures and the Equilibrium Condensation Sequence

The heavy curve in Figure 2 shows the temperature at the equator of the contracting proto-Saturnian cloud plotted against cloud size R_n, expressed in units of R_S. It defines the temperature of each gas ring at the moment of detachment from the cloud. The broken curves in the diagram define the equilibrium condensation temperatures $T_{i,0}$ of the prinicipal low-temperature chemical species which can form solar material, based on the condensation formalism developed by Lewis (1972). In computing these graphs we have assumed that the mass fractions $Z_{i,S}$ of the chemical species in the proto-Saturnian cloud occur in the same relative proportions as those which arise in solar material, but reduced by a factor 0.3 as described below. The solar abundances $Z_{i,\odot}$ are

listed in Table I, based on the compilation of Ross and Aller (1976) and augmented with the measurements of Lambert (1978) and Lambert and Luck (1978).

The condensation temperatures $T_{i,0}$ are computed for the pressure p_n on the mean orbit of the gas ring according to the vapour pressure equations

$$\log_{10} p_i(0) = \log_{10}(Z_{i,S} p_n \mu/\mu_i) = B_i - A_i/T_{i,0}, \tag{14}$$

where $\mu_i, p_i(0)$ denote the molecular weight and partial pressure of the i-th species and A_i, B_i are thermodynamic constants. They are listed in Table I and were derived from the date of Miller (1961), Delsemme and Wenger (1970) and Haudenschild (1971). NH_3 condenses directly from the gas at temperatures $\simeq 20$ K below the $NH_3 \cdot H_2O$ solidus. We discuss the implications of these results in Section 4.3.

4.2. Heavy Element Mass Fraction of the Proto-Saturnian Cloud

The mass of the gas ring shed at Rhea's orbit is 5.65×10^{26} g. This implies a total mass fraction of condensable rocks and ices of 9.3×10^{24} g, assuming solar abundances. Since the actual mass of Rhea is 2.49×10^{24} g (Tyler *et al.*, 1981), it follows that the actual mass fractions $Z_{i,S}$ of the condensable species in the proto-Saturnian cloud were reduced relative to the solar values by a factor of 0.3. Prentice (1981a) proposed that this shortfall is a natural consequence of the formation of Saturn's dense rock-ice core from the gas ring which was shed by the protosun at Saturn's orbit. The formation of such a core, consisting of rock, H_2O and NH_3 ice would, of course, result in the exhaustion of these species in the protosolar gas ring, prior to its capture. Thus with the exception of the uncondensing CH_4 and Ar, which are expected to be present in normal solar proportions, we propose that

$$Z_{i,S} \simeq 0.3 Z_{i,\odot}. \tag{15}$$

4.3. Chemical Compositions of the Satellites

The expected chemical composition of each satellite follows from inspection of Figure 2. We see that the icy satellites divide themselves into 3 main compositional classes, depending on the orbital distance from Saturn. Class I satellites correspond to objects consisting of rock and water ice. Mimas and Enceladus belong to this class. Class II objects, which include Tethys and Dione, consist of rock, H_2O ice and NH_3 ice (which is present as NH_3 hydrate in Tethys). Class III bodies contain rock, H_2O ice, NH_3 ice and CH_4 ice (incorporated as $CH_4 \cdot 5.75\, H_2O$).

The actual mass fractions f_i of the different chemical species in each satellite are given in Table II. They have been computed on the basis of considering the net contribution from each portion of the gas ring at the time of detachment from the parent cloud. It is implicitly assumed that the rate of accretion of each satellite is very much less than the rate of contraction of the cloud, so that the satellites are formed one at a time, commencing with Iapetus. We return to this point in Section 5.

From Equations (6) and (14) we see that the partial pressure p_i of a given chemical

TABLE II

Gas ring characteristics and the computed satellite compositions and densities

Satellite		Orbit radius	Gas ring density	Gas ring temperature		Gas pressure	Condensate mass fractions				Satellite densities ($g\,cm^{-3}$)		
											Theoretical		Observed
Name	Radius (km)	R_n/R_S	($g\,cm^{-3}$)	T_n(K)	T_n^*(K)	p_n(bar)	f_{rock}	f_{H_2O}	f_{NH_3}	f_{CH_4}	ρ_{uncomp}	ρ_{comp}	ρ_{obs}
1980 S28	~ 15	2.282	8.9(–4)	275	275	9.2	0.86	0.14	–	–	2.46	2.46	–
1980 S27 1980 S26	~ 50	~ 2.33	8.8(–4)	275	275	9.0	0.86	0.14	–	–	2.46	2.46	–
1980 S3 1980 S1	~ 100	~ 2.51	8.2(–4)	274	274	8.4	0.86	0.14	–	–	2.46	2.46	–
Mimas	197 ± 3	3.075	5.4(–4)	241	241	4.84	0.425	0.575	–	–	1.347	1.349	1.42 ± 0.18
Enceladus	251 ± 5	3.946	2.5(–4)	188	188	1.79	0.377	0.623	–	–	1.283	1.286	1.15 ± 0.55[c]
Tethys	525 ± 10(V1)[a]	4.884	1.3(–4)	152	153	0.76	0.351	0.582	0.067	–	1.239	1.246	1.25 ± 0.17
	530 ± 10(V2)												1.21 ± 0.16
Dione	560 ± 5	6.256	6.3(–5)	119	121	0.28	0.347	0.575	0.078	–	1.232	1.243	1.43 ± 0.06[c]
Rhea	765 ± 5	8.737	2.2(–5)	85	90	0.075	0.347	0.575	0.078	–	1.232	1.328	1.33 ± 0.09
							0.320	0.529	0.072	0.079	1.107	1.161	
Iapetus	730 ± 10	11.36[b]	9.3(–6)	65	75	0.026	0.319	0.527	0.072	0.082	1.103	1.145	1.16 ± 0.09

[a] V1 = Voyager 1, V2 = Voyager 2.

[b] Assumed original orbital radius.

[c] Based on non-Voyager masses (Kozai, 1976).

species, denoted by index i, varies with distance ξ from the mean orbit of the gas ring, of orbital radius R_n according as

$$p_i(\xi) = Z_{i,S} p_n(\mu/\mu_i) \exp(-\tfrac{1}{2}\alpha_n^* \xi^2/R_n^2), \tag{16}$$

where $\alpha_n^* = \mu G M_n/\mathscr{R} T_n^* R_n$. Condensation occurs only for radii $\xi < \xi_i$ where ξ_i is the solution of the equation

$$\log_{10} p_i(\xi_i) = B_i - A_i/T_n^*. \tag{17}$$

Rock is assumed to be fully condensed for the temperatures of interest in the present study. It is assumed to form a hydrous silicate, with water fraction 14%, in regions where ice is unable to condense directly (cf. Ransford *et al.*, 1981).

The effective condensing mass fraction of species i is then

$$z_{i,S} = Z_{i,S}[1 - \exp(-2.3026 A_i(1/T_n^* - 1/T_{i,0}))], \tag{18}$$

where $T_{i,0}$ is defined by Equation (14). If $T_{i,0} < T_n^*$ then $z_{i,S} = 0$. The fraction of water incorporated through the formation of hydrated silicate needs to be included in the count for $z_{1,S}$. Lastly, the normalized mass fractions f_i are given

$$f_i = z_{i,S} \Big/ \sum_{i=0}^{3} z_{i,S}. \tag{19}$$

A plot of f_i versus orbital radius R_n appears in Figure 3, whilst the values for the individual satellites are listed in Table II. We observe that the rock mass fraction steadily increases with decreasing orbital radius through the region of the satellite system. This trend is due to the steadily increasing temperature of formation $T_n \propto 1/R_n$ with decreasing cloud size. Iapetus is thus the least rocky of the satellites and Mimas the rockiest.

Because the incorporation of $NH_3 \cdot H_2O$ and $CH_4 \cdot 5.75\ H_2O$ ices cannot occur interior to orbital radii of 4.4 R_S and 6.9 R_S, respectively, Enceladus turns out to have the highest H_2O ice mass fraction of all the satellites. It is probably no coincidence, therefore, that this moon has the highest albedo of all the Saturnian satellites, with Tethys, the next most watery moon, being the 2nd brightest. That is, the lower albedo of Mimas compared to its neighbours Enceladus and Tethys comes about simply because of its higher rock fraction. The measured density of Mimas of $1.42 \pm 0.18\ \mathrm{g\,cm^{-3}}$ (Tyler *et al.*, 1982; Davies and Katayama, 1983) implies a rock fraction of 47%.

Between orbital radii of 1.9 R_S and 2.8 R_S the temperature at the equator of the contracting cloud exceeds the H_2O ice-point. This implies that the smaller inner moonlets 1980 S1, 1980 S3, 1980 S26, 1980 S27, and 1980 S28 should all consist largely of hydrated silicates. The lower albedo of these bodies compared to Mimas (Smith *et al.*, 1982) supports this conclusion. The particles of the A and F rings are also expected to consist mostly of rock.

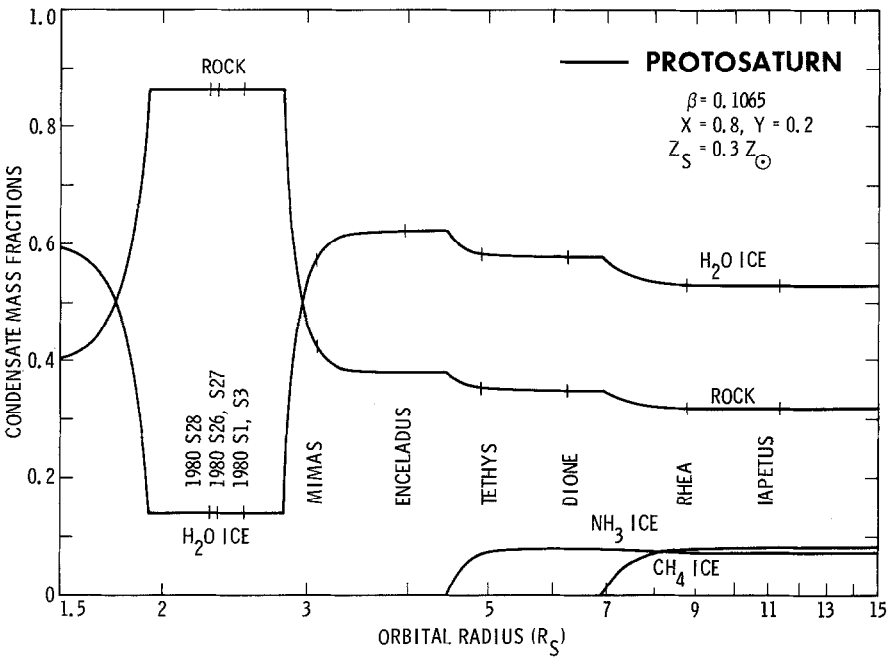

Fig. 3. Expected mass fractions of the main condensing constituents in the system of detached gaseous rings, plotted as a continuous function of orbital radius. The line for H_2O ice includes the contribution of water of hydration. Water is incorporated into the rock to form serpentine in regions where it is unable to condense directly from the gas. CH_4 is incorporated into the condensate mix through the formation of the clathrate $CH_4 \cdot 5.75H_2O$.

4.4. SATELLITE DENSITIES

The uncompressed density of the condensate material is given by the equation

$$1/\rho_{\text{unc}} = \sum_{i=0}^{3} f_i/\rho_i, \tag{20}$$

where ρ_i denotes the intrinsic density of species i. Values of ρ_i at the present-day temperature $T_S = 77$ K at Saturn's orbit are listed in Table I (Lupo and Lewis, 1979, 1980; Stewart, 1960). The density of anhydrous rock has been taken from Lupo (1982). The density of $NH_3 \cdot H_2O$ is taken to be the molar average of the densities of H_2O and NH_3 ices. This is a fairly unimportant assumption since beyond orbital radius 5.3 R_S and NH_3 condenses directly from the gas, anyway. Tethys condenses just inside the stability field of NH_3 hydrate. CH_4 is assumed to have separated out from the clathrate structure in the present satellite, as discussed below.

A plot of ρ_{unc} versus orbital radius R_n appears in Figure 4. We observe that ρ_{unc} steadily decreases with increasing distance through the region of the satellite system. The decrease takes place in a step-wise manner from one plateau level to the next as the

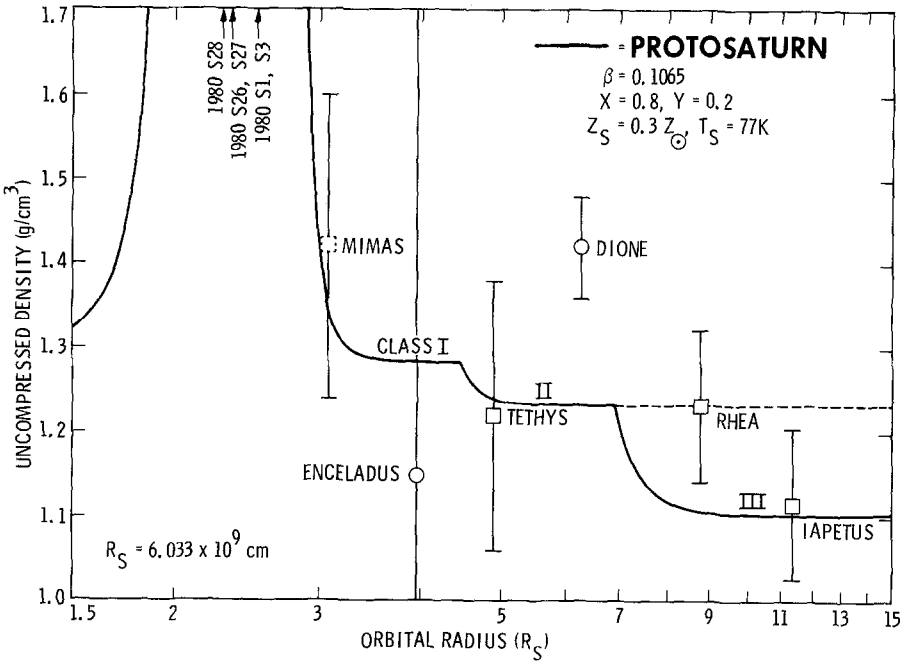

Fig. 4. Uncompressed density of the solid condensate versus orbital radius, based on the relative mass fractions of the chemical constituents given in Figure 3. The theoretical density function (heavy line) changes sharply with orbital distance at points where the stability field of the various low temperature ices (H_2O, $NH_3 \cdot H_2O$ and $CH_4 \cdot 5.75H_2O$) are first entered. The observed uncompressed densities of the satellites are also plotted. Squares correspond to Voyager-determined values and circles to estimates based on non-Voyager masses (Tyler *et al.*, 1982). All densities are computed for the present temperature $T_S = 77$ K at Saturn's orbit.

equilibrium stability field of the different ices H_2O, $NH_3 \cdot H_2O$, and $CH_4 \cdot 5.75\ H_2O$, denoted by classes I, II, and III are entered. Also marked on the diagram are the observed satellite densities ρ'_{obs} after the effects of self-compression due to gravity have been removed. We have $\rho'_{obs} = \rho_{obs} - \Delta\rho_{grav}$ where ρ_{obs} are the actual densities and $\Delta\rho_{grav} = \rho_{comp} - \rho_{unc}$ is the difference between the theoretical compressed and uncompressed density of a satellite whose composition is defined by the model above and whose radius equals the observed Voyager mean (Smith *et al.*, 1981, 1982; Davies and Katamaya, 1983). The values of ρ_{comp} and ρ_{unc} appear in Table II. It is assumed that the satellite interiors are chemically homogeneous. Date on the compressibility of rock and ices are taken from Lupo and Lewis (1979, 1980). Thermal expansion due to radiogenic heating is ignored since it produces less than 1% change in density at the centre of a satellite of radius 700 km (Consolmagno and Lewis, 1978).

We observe that the theoretical density curve ρ_{unc}, lies well inside the error bounds for Mimas, Tethys and Iapetus. That is, Voyager 2 has confirmed the predictions of the model in these instances (Prentice, 1981a, b, c; cf. Tyler *et al.*, 1982). The density of

Rhea, however, appears to lie outside the value expected for its condensation class. Instead a class II composition seems more compatible with the Voyager data (Tyler *et al.*, 1981), suggesting that Rhea has somehow lost its primordial share of CH_4 if the above model is correct. We return to this point in Section 5.

It is clear from Figure 4 that Dione is far too dense to fit as a class II object. The mass of this moon, however, has not been measured by Voyager but instead taken from a simplified theory of the Dione-Enceladus orbit resonance (Kozai, 1976). We therefore suggest, along with Tyler *et al.* (1982), that future space measurements may yield a much lower mass for Dione that will bring its density into line with the condensation value. On the basis of the Voyager measured radius of 560 ± 5 km we predict a mass for Dione of $(9.1 \pm 0.3) \times 10^{23}$ g. By the same token, if Enceladus truly is a class I object, consisting of 38% rock and 62% water ice, its mass should be $(8.5 \pm 0.5) \times 10^{22}$ g for a Voyager radius (251 ± 5) km (Davies and Katamaya, 1983).

5. Timescales of Satellite Formation and Post-Accretional Evolution of the Satellites

5.1. TIMESCALES

The physical processes governing the accumulation of the condensate material in gaseous rings has been examined in detail by Hourigan (1977, 1981a, b), Hourigan and Prentice (1979), Prentice and ter Haar (1979a) and Prentice (1978a, 1980c). As soon as a grain has condensed from the gas it begins to settle towards the mean orbit of the gas ring, as schematically illustrated in Figure 1. Its distance ξ from the mean circular orbit R_n decreases with time t according to the equation

$$\xi(t) = \xi_0 \exp(-\omega_n^2 t/\gamma_1), \tag{21}$$

where

$$\gamma_1 = 1.62\rho_n\lambda_n(8\mathscr{R}T_n/\pi\mu)^{1/2}/\rho_{gr}a_{gr}^2 \tag{22}$$

is the linear Stokes drag coefficient. Here ρ_{gr} (g cm^{-3}) and a_{gr} (cm) denote the grain density and radius and $\lambda_n \simeq 2.0 \times 10^{-9}/\rho_n$ cm is the mean molecular path length in the gas (Williams and Crampin, 1971). This yields a time-scale for settling out

$$t_{set} = \frac{\gamma_1}{\omega_n^2} = 0.33\tau_{orb}(R_n/R_S)/\rho_{gr}a_{gr}^2 \text{ s}, \tag{23}$$

where τ_{orb} denotes the Kepler orbital period at radius R_n and we have eliminated T_n using Equations (7) and (11).

Once sufficient material has settled onto the mean circular orbit R_n it begins to aggregate under the influence of its own gravity forming isolated satellitesimals. The time-scale for this process is

$$t_{agg} \simeq \tau_{orb}(M_S/m_{set})^{1/2}, \tag{24}$$

where m_{set} denotes the mass of settled material. The process governing the aggregation of satellitesimals into a single planetary embryo is fairly complex and is not considered

here. Hourigan's (1981b) calculations for the planetary system indicate that most of the accumulation will have been completed in a time of order $10^2\ t_{agg}$.

The remaining time-scale we consider here is that governing the rate of contraction of the parental globe, of equatorial radius R_e. Assuming Kelvin–Helmholtz equilibrium we have

$$t_{con} = R_e/\dot{R}_e = C_e G M_n^2/2.82\pi\sigma_S R_e^3 T_e^4, \tag{25}$$

where $C_e GM_n^2/R_e$ denotes the excess gravitational potential energy of the cloud and C_e is a constant of order unity (Prentice, 1978b). Integration of Equation (25) yields the times t_n at which the cloud contracts through the satellite positions R_n commencing from the initial radius $R_0 = 11.36\,R_S$.

The values of t_{set}, t_{agg}, and t_n for each of the major satellites are listed in Table III. In evaluating t_{set} we have put m_{set} equal to the observed satellite mass m_{obs}, which is shown in Table III (Tyler *et al.*, 1981, 1982).

TABLE III

Timescales governing satellite accumulation

Satellite	Mass (10^{23} g)	Orbit period τ_{orb} (d)	Grain settling time[b] t_{set} (yr)	Aggregation time $10^2\ t_{agg}$ (yr)	Gas ring detachment time, t_n (yr)
Mimas	0.455 ± 0.054	0.942	20	900	1.98(8)
Enceladys	0.76 ± 0.36	1.370	40	1000	1.77(8)
Tethys	7.55 ± 0.90	1.888	70	450	1.54(8)
Dione	10.52 ± 0.33	2.737	130	550	1.21(8)
Rhea	24.9 ± 1.5	4.518	300	600	6.1(7)
Iapetus	18.82 ± 1.2	6.70[a]	600	1000	0

[a] Assumed initial orbit period.

[b] Calculated for $a_{gr} = 0.01$ cm, $\rho_{gr} = 1.2$ g cm^{-3}.

We observe from the table that the times taken for settling out of the grain material and its subsequent accumulation along the mean orbit of the gas ring to form a satellite are very much less than the times taken for the proto-Saturnian cloud to contract from one orbital position to the next. Typically $t_{set} \sim 10^2$ yr and $10^2\ t_{agg} \sim 10^3$ yr compared to the time interval $\Delta t_n \sim 3 \times 10^7$ yr between successive gas ring detachments. The satellites, therefore, are formed literally one at a time, commencing with the outermost one – Iapetus.

5.2. Mass Distributions of the Inner Satellites and the Physical Lifetimes of the Gas Rings

According to Equation (4) the masses of the gas rings are all about the same, namely 5.6×10^{26} g for $\langle R_n/R_{n+1}\rangle = 1.30$, $M = M_S$ and $f = 0.007$. A question therefore arises

as to why the masses of the satellites are not all the same or, at least, bear much the same proportion as the mass fraction of condensates appropriate to their compositional class. Prentice and ter Haar (1979a) pointed out that the Galilean satellites do, by and large, properly reflect the total mass of condensate that was available in each of their formative gas rings. The masses of Rhea and Iapetus are roughly comparable. Interior to the orbit of Rhea, however, the satellite masses show a systematic decline moving towards Saturn.

The decline in the mass distribution of the inner Saturnian satellites can probably be linked with the onset of destructive dynamical mixing between the closely spaced gas rings. From Equation (5) we see that there is a large discontinuity in the orbital angular velocity distribution $\omega(s, z)$ of the gas in crossing the cylindrical interface $s = R_{\text{int}} = (R_n R_{n-1})^{1/2}$ from the n-th to the $(n-1)$-th gas ring. If ρ_{int} denotes the gas density at the interface between these rings, it follows from Equation (6) that

$$\rho_{\text{int}}/\rho_n = \exp\left(-\tfrac{1}{2}\alpha_n[\sqrt{R_{n-1}/R_n} - 1]^2\right) \tag{26}$$

$$= \begin{cases} 0.11, & \text{Saturn;} \\ 8 \times 10^{-4}, & \text{Jupiter;} \end{cases}$$

noting $\alpha_{n\text{S}} \simeq 225$, $\alpha_{n\text{J}} \simeq 175$, $\langle R_{n-1}/R_n \rangle_{\text{J}} = 1.65$. Thus in the case of the proto-Jovian cloud, where the relative spacings between the gas rings is large, the gas density at the interface is so low that mixing is probably unimportant. For Saturn, however, ρ_{int}/ρ_n is not very small and so mixing across the interface will lead to an early breakdown in the angular velocity distribution (5). This distribution is also the one which is responsible for the efficient focussing of the condensate grains onto the mean orbit R_n of the gas ring.

We therefore conclude that the masses of Saturn's moons simply reflect the mass of material which safely settled onto the mean orbit of the respective gas rings, before the latter were disrupted. It follows from Table III that the lifetimes of the gas rings are probably of order only 10^2–10^3 yr.

5.3. FORMATION OF TITAN

Titan is 60 times too massive for it to be a natural moon of Saturn, if our interpretation of Equation (4) is correct. In addition, it has an orbital radius of $20.25\,R_{\text{S}}$ which lies well outside the limit $12.3\,R_{\text{S}}$, given by Equation (13), where the proto-Saturnian cloud first identified itself thermodynamically. We therefore suggest, as first proposed by Prentice (1980a), that Titan is actually a captured moon of Saturn. It condensed as a secondary embryo in the gas ring that was shed by the protosun at Saturn's orbit. That being the case, it would be expected to consist chiefly of rock, H_2O ice and NH_3 ice. Voyager 1 found that Titan did, indeed, have a density very similar to Callisto, a moon of the same proposed composition (Prentice and ter Haar, 1979b). Moreover Titan's atmosphere was found to consist mostly of N_2, rather than CH_4, again supporting an origin in a much warmer environment than is provided by the cool environs of the proto-Saturn cloud at that radius (see Figure 2; cf., Tyler *et al.*, 1981).

Consider then the possible capture of Titan in a circumplanetary gaseous disk extending

from radius 12.3 R_S out to, say, 60 R_S. Such a disk could have been shed by the rotating proto-Saturnian cloud prior to contracting to radius 11.4 R_S where the process of shedding gas rings commenced. The processes governing satellite capture in a gaseous disk have been explored by Pollack *et al.* (1979). The characteristic timescale for gas drag to arrest the motion of a body of radius a_T and density ρ_T and bring it into a circular co-moving orbit of radius R_n in a gaseous Keplerian disk of density ρ_g has been estimated by Prentice (1978a) to be

$$t_{cap} \simeq \tau_{orb}\rho_T a_T/\rho_g R_n \simeq 350\,\text{yr}. \tag{27}$$

In calculating this value, we have set $\rho_T = 1.88\,\text{g cm}^{-3}$, $a_T = 2575\,\text{km}$, $R_n = 20.25\,R_S$ and $\rho_g = 5 \times 10^{-7}\,\text{g cm}^{-3}$, noting the gas density in the disk to be about 0.3 times the corresponding value of a gas ring centred on that radius. We conclude that as t_{cap} is very small compared to the evolutionary lifetime of the cloud t_{con}, a gas drag capture origin for Titan is indeed a physically viable possibility.

5.4. THE PRESENT ORBIT OF IAPETUS

Ward (1981) has pointed out that the close similarity of the sizes of Iapetus and Rhea suggests that Iapetus is a naturally formed moon of Saturn. We suggest, therefore, that Iapetus is the missing satellite which condensed from the first shed gaseous ring at orbital radius 11.4 R_S.

Soon after its formation, and before the proto-Saturnian cloud had contracted to the orbit of Rhea, we proposed that Titan entered the Saturnian system. During Titan's first few passages around the cloud, whilst the orbit was still very irregular, we propose that a near encounter of Titan with Iapetus took place. Iapetus was dislodged from its inner orbit and followed Titan into the outer reaches of the circumplanetary disk, where gas drag trapped it into a new, but distant, circular orbit. The unusual orbital inclination of Iapetus is probably due to a warping of the outer fringes of the gaseous disk by solar torques, as shown by Ward. Saturn has an obliquity of 26.7°.

5.5. THERMAL EVOLUTION OF THE ICY SATELLITES

Figure 5 shows the temperature at the orbital positions of each of the satellites, plotted as a function of time elapsed after the proto-Saturnian cloud shed its first gas ring at orbital radius 11.4 R_S. The heavy curves defines the surface temperature of the contracting cloud. The points at which the satellites are formed are indicated by circles on this curve.

We observe that Rhea condenses very close to the CH_4 triple point (90.7 K). Some 3×10^7 yr after its formation, Rhea's temperature rose above this point causing the CH_4 in equilibrium with the clathrate to liquefy. If there are any fissures or flaws in the satellite mantle, as Voyager photographs do indeed indicate (Smith *et al.*, 1981), the CH_4 will rise to the satellite surface and evaporate away. We assume that Rhea's formative gas ring will have long since dispersed by that stage. For this reason Rhea is now expected to consist only of rock, H_2O ice and NH_3 ice, as indicated in Table II. Certainly the observed density is consistent with this hypothesis!

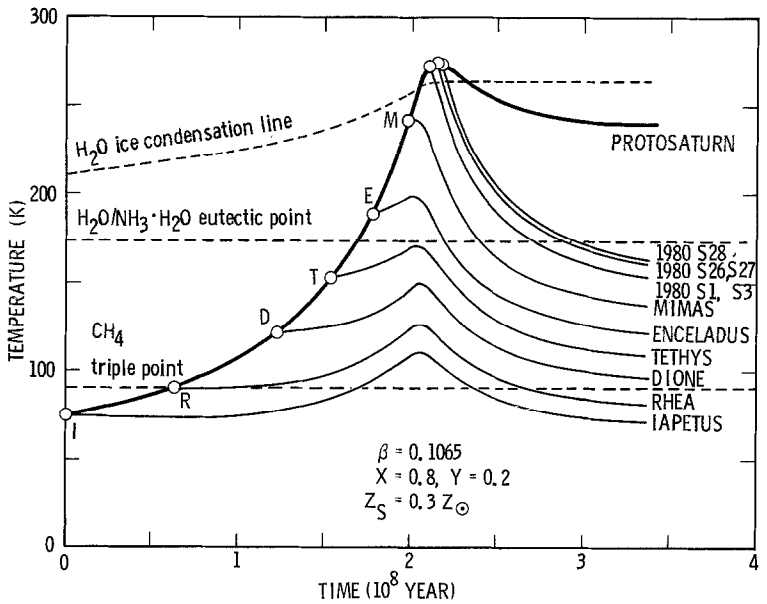

Fig. 5. The surface temperature of the proto-Saturnian cloud and the temperatures of its family of embryonic moons, plotted against elapsed time from the initial cloud size of 11.4 R_S. The time and temperature of formation of each satellite are indicated by the small circles. The minimum temperatures at which melting of solid CH_4 and $NH_3 \cdot H_2O$ can occur are also marked.

The Voyager-determined density of Iapetus of $1.155 \pm 0.09\ g\,cm^{-3}$ is consistent with this body having retained its primordial share of CH_4. Had this body remained in its proposed orbit of formation, at 11.4 R_S, however, this would certainly not have been the case, as we see from Figure 5. Iapetus would have experienced the same fate as Rhea.

The low density of Iapetus thus adds weight to our conjecture that this satellite was transferred to its present orbital radius of 59 R_S within the first 6×10^7 yr of its existence. Radiogenic heating will eventually cause the temperature throughout most of the interior of this satellite to rise above the CH_4 triple point (Consolmagno and Lewis, 1978). Most of the CH_4, therefore, may have separated out from the clathrate structure to form a layer of solid CH_4 lying not far below the satellite's frozen outer mantle. We suggest here that the dark markings observed on the leading hemisphere of this satellite are organic tars. Perhaps they were formed through highly energetic impacts of post-accretional debris on the satellite's methane-rich sub-structure.

The remaining point to make concerns Tethys. Some 5×10^7 yr after its formation, the temperature at Tethys' orbit rose to within 2 K of the $H_2O/NH_3 \cdot H_2O$ eutectic point. Coupled with a modest rise of temperature due to radiogenic heating (Consolmagno and Lewis, 1978) it would seem almost certain that the interior of this satellite melted at this time, causing the rock constituent to sink to the centre. This satellite therefore probably has a central rocky core covering some 35% of its mass.

6. Conclusions

We have proposed that each of Saturn's regular satellites, except Titan, condensed from an orbiting system of gaseous rings which had been shed at the equator of the primitive rotating cloud which contracted gravitationally to form Saturn. If the cloud possessed the same level of turbulent stress as the clouds which formed Jupiter and the sun, then the mean satellite densities predicted by the model coincide in each instance with the values measured by the Voyager spacecraft.

We have shown that the uncompressed satellite densities and rock mass fractions steadily increase towards the planet as a result of the formation temperature T_n varying inversely with orbital radius R_n, as $T_n \propto 1/R_n$. This same temperature law is also reflected in the chemical composition of both the planetary system and the regular satellite system of Jupiter (Lewis, 1974; Prentice and ter Haar, 1979b). It is a natural outcome of the proposed hypothesis of a uniform gravitational contraction taking place amongst all protoplanetary clouds.

We have suggested that Titan is a captured satellite of Saturn, which formed as a secondary embryo in the gas ring that was shed by the protosolar cloud at Saturn's orbit. Iapetus was the first formed moon of Saturn. It originally occupied an orbit near $11.4\,R_S$ and was driven out to its present position as a result of Titan's dynamic capture. Some 8% of the mass of Iapetus consists of solid methane ice, accounting for the low density of this satellite. In contrast, the innermost moonlets of Saturn should consist mostly of hydrated silicates and have a density close to $2.4\,\mathrm{g\,cm^{-3}}$ (Prentice, 1980b). Saturn's family of moons thus form a remarkably diverse group of objects.

Acknowledgements

Part of the research reported here was performed during tenure of a NRC-NASA Senior Research Associateship at the Jet Propulsion Laboratory. I am very grateful to Dr J. D. Anderson for his generous hospitality and support at JPL. Travel funds to attend the Tucson meeting were provided by the Ian Potter Foundation (Melbourne). Useful discussions with R. D. Brown, P. D. Godfrey, K. Hourigan, and J. S. Lewis are acknowledged.

References

Anderson, J. D., Null, G. W., Biller, E. D., Wong, S. K., Hubbard, W. B., and MacFarlane, J. J.: 1980, *Science* **207**, 449.

Cohen, M.: 1981, *Nature* **291**, 611.

Consolmagno, G. J. and Lewis, J. S.: 1978, *Icarus* **34**, 280.

Cox, J. P. and Giuli, R. T.: 1968, *Principles of Stellar Structure*, Vol. 1. Gordon and Breach, New York.

Davies, M. E. and Katayama, F. Y.: 1983, *Icarus* **53**, 332.

Delsemme, A. H. and Wenger, A.: 1970, *Planetary Space Sci.* **18**, 709.

Fouché, M.: 1884, *Compt. Rend. Acad. Sci.* **99**, 903.

Gautier, D., Conrath, B. J., Flasar, F. M., Hanel, R. A., and Kunde, V. G.: 1981, *J. Geophys. Res.* **86**, 8713.

Grossman, A. S., Pollack, J. B., Reynolds, R. T., Summers, A. L., and Graboske, H. C.: 1980, *Icarus* **42**, 358.
Haudenschild, C.: 1971, *JPL Space Programs Summary 37-64*, Vol. III, pp. 4–9. Jet Propulsion Laboratory, Pasadena.
Herbig, G. H.: 1962, *Advances in Astron. Astrophys.* **1**, 47.
Hourigan, K.: 1977, *Proc. Astron. Soc. Australia* **3**, 169.
Hourigan, K.: 1981a, *Proc. Astron. Soc. Australia* **4**, 226.
Hourigan, K.: 1981b, Ph.D. Thesis, Monash University (Clayton, Victoria).
Hourigan, K. and Prentice, A. J. R.: 1979, *Proc. Astron. Soc. Australia* **3**, 389.
Hoyle, F.: 1960, *Quart, J. Roy. Astron. Soc.* **1**, 28.
Hubbard, W. B. and MacFarlane, J. J.: 1980, *J. Geophys. Res.* **85**, 225.
Jeans, J. H.: 1928, *Astronomy and Cosmogony*, Cambridge University Press, Cambridge.
Kozai, Y.: 1976, *Publ. Astron. Soc. Japan* **28**, 675.
Lambert, D. L.: 1978, *Monthly Notices Roy. Astron. Soc.* **182**, 249.
Lambert, D. L. and Luck, R. E.: 1978, *Monthly Notices Roy. Astron. Soc.* **183**, 79.
Laplace, P. S. de: 1796, *Exposition du Systéme du Monde*, Courcier, Paris.
Lewis, J. S.: 1972, *Icarus* **16**, 241.
Lewis, J. S.: 1974, *Science* **186**, 440.
Lupo, M. J.: 1982, *Icarus* **52**, 40.
Lupo, M. J. and Lewis, J. S.: 1979, *Icarus* **40**, 157.
Lupo, M. J. and Lewis, J. S.: 1980, *Icarus* **42**, 29.
Miller, S. L.: 1961, *Proc. Nat. Acad. Science* **47**, 1798.
Pollack, J. B., Grossman, A. S., Moore, R., and Graboske, H. C.: 1976, *Icarus* **29**, 35.
Pollack, J. B., Burns, J. A., and Tauber, M. E.: 1979, *Icarus* **37**, 587.
Prentice, A. J. R.: 1973, *Astron. Astrophys.* **27**, 237.
Prentice, A. J. R.: 1974, in *In the Beginning . . .*, J. P. Wild (ed.), Australian Academy of Science, Canberra, pp. 15–47.
Prentice, A. J. R.: 1976, *Astron. Astrophys.* **50**, 59.
Prentice, A. J. R.: 1978a, in *The Origin of the Solar System* S. F. Dermott (ed.), John Wiley & Sons, London, pp. 111–162.
Prentice, A. J. R.: 1978b, *The Moon and the Planets* **19**, 341.
Prentice, A. J. R.: 1980a, *JPL Publication 80-80*, Jet Propulsion Laboratory, Pasadena.
Prentice, A. J. R.: 1980b, *Phys. Lett.* **80A**, 205.
Prentice, A. J. R.: 1980c, *Australian J. Phys.* **33**, 623.
Prentice, A. J. R.: 1981a, *JPL Publication 81-79*, Jet Propulsion Laboratory, Pasadena.
Prentice, A. J. R.: 1981b, *Proc. Astron. Soc. Australia* **4**, 164.
Prentice, A. J. R.: 1981c, *Bull. Amer. Astron. Soc.* **13**, 743.
Prentice, A. J. R.: 1983, *Australian Physicist* **20**, 37.
Prentice, A. J. R. and ter Haar, D.: 1979a, *The Moon and the Planets* **21**, 43.
Prentice, A. J. R. and ter Haar, D.: 1979b, *Nature* **280**, 300.
Ransford, G. A., Finnerty, A. A., and Collerson, K. D.: 1981, *Nature* **289**, 21.
Ross, J. E. and Aller, L. H.: 1976, *Science* **191**, 1223.
Slattery, W.: 1977, *Icarus* **32**, 58.
Smith, B. A. *et al.*: 1981, *Science* **212**, 169.
Smith, B. A. *et al.*: 1982, *Science* **215**, 504.
Stewart, J. W.: 1960, *J. Chem. Phys.* **33**, 128.
Stone, E. C. and Miner, E. D.: 1982, *Science* **215**, 499.
ter Haar, D.: 1967, *Ann. Rev. Astron. Astrophys.* **5**, 267.
Tyler, G. L., Eshleman, V. R., Anderson, J. D., Levy, G. S., Lindal, G. F., Wood, G. E., and Croft, T. A.: 1981, *Science* **212**, 201.
Tyler, G. L., Eshleman, V. R., Anderson, J. D., Levy, G. S., Lindal, G. F., Wood, G. E., and Croft, T. A.: 1982, *Science* **215**, 553.
Ward, W. R.: 1981, *Icarus* **46**, 97.
Williams, I. P. and Crampin, D. J.: 1971, *Monthly Notices Roy. Astron. Soc.* **152**, 261.